SCIENTIFIC REPORTS

OPEN

SUBJECT AREAS:
NANOBIOTECHNOLOGY
MAGNETIC MATERIALS
NANOPARTICLES
BIOMIMETIC SYNTHESIS

Received
6 August 2012

Accepted
2 October 2013

Published
21 October 2013

Correspondence and requests for materials should be addressed to S.-H.Y. (shyu@ustc.edu.cn)

* These authors contributed equally to this work.

Bioinspired greigite magnetic nanocrystals: chemical synthesis and biomedicine applications

Mei Feng*, Yang Lu*, Yuan Yang, Meng Zhang, Yun-Jun Xu, Huai-Ling Gao, Liang Dong, Wei-Ping Xu & Shu-Hong Yu

Division of Nanomaterials and Chemistry, Hefei National Laboratory for Physical Sciences at Microscale, Department of Chemistry, Department of Materials Science and Engineering, Collaborative Innovation Center of Suzhou Nano Science and Technology, University of Science and Technology of China, Hefei, Anhui 230026, P. R. China.

Large scale greigite with uniform dimensions has stimulated significant demands for applications such as hyperthermia, photovoltaics, medicine and cell separation, etc. However, the inhomogeneity and hydrophobicity for most of the as prepared greigite crystals has limited their applications in biomedicine. Herein, we report a green chemical method utilizing *β*-cyclodextrin (*β*-CD) and polyethylene glycol (PEG) to synthesize bioinspired greigite (Fe_3S_4) magnetic nanocrystals (GMNCs) with similar structure and magnetic property of magnetosome in a large scale. *β*-CD and PEG is responsible to control the crystal phase and morphology, as well as to bound onto the surface of nanocrystals and form polymer layers. The GMNCs exhibit a transverse relaxivity of 94.8 $mM^{-1}s^{-1}$ which is as high as iron oxide nanocrystals, and an entrapment efficiency of 58.7% for magnetic guided delivery of chemotherapeutic drug doxorubicin. Moreover, enhanced chemotherapeutic treatment of mice tumor was obtained via intravenous injection of doxorubicin loaded GMNCs.

Since the discovery of magnetite nanocrystals (NCs) in magnetotactic microorganism[1–3], magnetic magnetosome containing either magnetite or greigite has attracted wide attention in the past years[4]. Interestingly in magnetotactic microorganism, the magnetic nanocrystals always existed in the form of 'magnetosome' through being surrounded by bilayer lipid membrane which is decorated by protein. Though most of the magnetosomes contain magnetite as a core[5,6], in the many-celled magnetotactic prokaryote an iron-sulphide biogenic mineral, namely greigite (Fe_3S_4) was found. These magnetosome can align the bacteria parallel to the direction of the geomagnetic field, and also plays an important role in the sulfur geochemical cycle and sediment magnetization[7]. Besides, some greigite minerals was found to function as hardening materials on the foot of a deep-sea snail[8]. Owing to these interesting findings, the greigite nanomaterials are expected to exhibit more interesting applications in the near future.

Magnetic nanomaterials have been widely investigated owing to their various promising applications, such as magnetic separation and ultrahigh density magnetic storage[9], catalysis[10], biomedicine[11–14], and sensors[15]. As an analogue of magnetite with ferromagnetic in inverse thiospinel of iron (AB_2S_4)[16], greigite NCs have been studied and utilized for hyperthermia[17,18]. Besides, it is reported that they can represent alternative materials in Li-ion batteries and serve as intermediates in photovoltaics[19,20]. Particularly, the nontoxic, magnetic iron sulfide nanocrystals show great potentials in medicine and cell separation[21]. It is therefore imperative to explore the interesting properties and applications of the magnetosome-like GMNCs. Recently, Fe_3S_4 nanocrystals have been obtained by several methods, such as bacteria-mediated biosynthesis[22], hydrothermal route[23,24], single-source precursor approach[21,25], and ionic liquid-modulated method[26]. However, most of them are complicated, and most of the as-prepared Fe_3S_4 nanocrystals are inhomogeneous and hydrophobic[21,22,24–27], which limit their applications in biomedicine. In addition, some byproducts, such as FeS_2, Fe_7S_8, and $Fe_{1-x}S$, would be formed as a small variation in stoichiometry can lead to huge changes in their properties. Therefore, it is important but challenging to find a way to synthesize pure and stable GMNCs.

Herein, using a facile solvothermal method, we have successfully obtained the magnetosome-like GMNCs with pure and stable phase in a large scale. Both *β*-CD and PEG have been employed to control the phase, shape and size of GMNCs and form protective layers outside the greigite core. Notably, the *β*-CD and PEG bicomponent layer can not only protect the magnetic core but also enhance the biocompatibility of these NCs, which would act

Table 1 | The samples prepared in the presence of different surfactants or stabilizers

reagents	Solvents	surfactants/stabilizers	magnetism (Y/N)	phase
$Fe(acac)_3$, TAA	EG	OA	Y	Fe_7S_8
		PEG#	Y	Fe_3S_4/Fe_7S_8
		CTAB	Y	Fe_3S_4/Fe_7S_8
		TOPO	Y	Fe_3S_4/Fe_7S_8
		PAM	Y	$Fe_{1-x}S/Fe_7S_8$
		L-Cystine	N	/
		SDS	N	/
		PVP	N	/

Note:PEG# stands for PEG4000. All chemical shortenings have been offset in Methods.

like the way of natural magnetosome membrane. With the perfect phase stability, water solubility and biocompatibility, the NCs are very suitable to be applied in the area of biomedicine, which is investigated in this paper including magnetic resonance imaging (MRI), drug delivery and even cancer inhibition. Moreover, owing to the similar polymer shell-core structure with natural magnetosome, we believe that these magnetosome-like GMNCs would have a bright future in biology and medicine.

Results

Large scale synthesis of magnetosome-like GMNCs. In a typical synthesis procedure, the iron (III) acetylacetonate ($Fe(acac)_3$), thioacetamide (TAA), β-CD and PEG were mixed orderly in ethylene glycol (EG) at 160°C for 2 h in the atmosphere of flowing nitrogen (see Methods). Afterwards, products with black color were obtained. Choosing appropriate surfactants or stabilizers is critically important in order to control the nucleation and growth, which will affect the crystal shapes of the obtained GMNCs. To obtain the Fe_3S_4 with high purity and stability, we have established a series of experiments investigating the effects of several different commonly used surfactants or stabilizers under the same condition, results of which were shown in Table 1. Obviously, neither other surfactants or stabilizers, nor PEG (4000) molecules solely could result in pure phase of Fe_3S_4. Cyclodextrins, including α, β, and γ-CD, have also been tried as they are regarded as structural and functional straightjacket, which can offer restrictive utility in terms of size, shape, and availability of chemically useful functional groups[28]. Interestingly, in spite of the large size and some sheet-like byproducts, pure phase of Fe_3S_4 nanocrystals was obtained only in the case of β-CD (see Supplementary Information, Fig. S1). Based on the investigations and for the purpose of bio-medicine applications, we tried the cooperation of the three kinds of cyclodextrins with PEG (4000) molecules. Noticeably, hybrid phases including monoclinic Fe_7S_8 and cubic Fe_3S_4 were observed (see Supplementary Information, Fig. S2), which illuminated that β-CD has played the key role during the whole synthesizing process, rather than α or γ-CD. In addition, we have analyzed the samples for different reaction time (0.5, 1.0 and 2.0 h) after the injection of TAA. A large number of small crystals were observed in the TEM images (see Supplementary Information, Fig. S3a and b), and XRD patterns (see Supplementary Information, Fig. S3c) of these samples within 1.0 h displayed weak crystallization with broaden peaks. According to the results and the observation of many polymers around the nanoparticles, we deduced that β-CD and PEG molecules would help to control the nucleation of the GMNCs. Based on the successful synthesis, pilot empirical chemical equations were given according to the basic chemical properties of the reactants (see Supplementary Information, Equation S1). We deduced that thioacetamide were hydrolyzed owing to the existence of hydrogen ion in the ethylene glycol solvent. At the same time, hydrogen sulfide came into being and reacted with iron ions. Finally, we obtained the Fe_3S_4 nanocrystals after the process. While chemical formula of magnetotactic bacteria has been discovered recently[29], we expect to carry out an in-depth investigation on the formation mechanism of our GMNCs in future. The reactions in this process, including the empirical chemical formula for the surface-coated GMNCs, would be systematically investigated in the future by using a series of characterization methods, such as electron paramagnanetic resonance (EPR), X-ray absorption fine structure (XAFS), X-ray photoelectron spectra (XPS). This would greatly assist in development of foundations to establish important correspondence, grounded in physical chemistry, natural and synthetically created bio-inspired materials.

By leveraging the cooperation of β-CD and PEG molecules, we have proposed a schematic illustration for the similarity between the natural magnetosome and the as-synthesized magnetosome-like GMNCs as shown in Fig. 1. Owing to the co-function of hydrophilic β-CD and PEG molecules around the surface of Fe_3S_4 magnetic cores, it is believed that the as-prepared GMNCs possessed pretty similar polymer shell-core structure and protection function to a natural magnetosome, namely the magnetosome-like GMNCs were achieved. Moreover, the water-solubility and biocompatibility of GMNCs have also been enhanced, which further confirmed the unique coordination of β-CD and PEG molecules during the whole synthesizing process.

Characterization and properties of the magnetosome-like GMNCs. The morphology and dimensions of the as-prepared GMNCs were examined by the typical field-emission scanning electron microscopy (FESEM) in Fig. 2a and transmission electron microscopy (TEM) in Fig. 2b. A large scale of homogeneous and monodisperse NCs with an average diameter of about 80–100 nm were observed and the average diameter was statistically obtained to be 90 ± 12 nm, which were similar to the biogenic greigite nanocrystals[4,7,23,30]. The phase and purity of the as prepared GMNCs were examined by X-ray diffraction

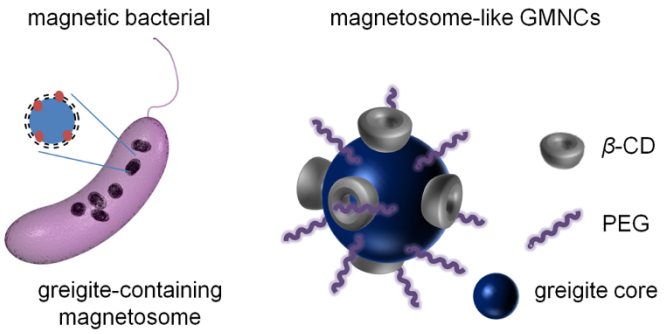

Figure 1 | Schematical illustration of the greigite-containing magnetosome and the chemical synthesized magnetosome-like GMNCs. Natural Greigite-containing magnetosomes with lipid bilayer are produced by the sulfate-reducing magnetic bacteria, while the synthesis of magnetosome-like GMNCs with similar protecting membrane is carried out in mild chemical conditions with the bound of β- CD and PEG molecules.

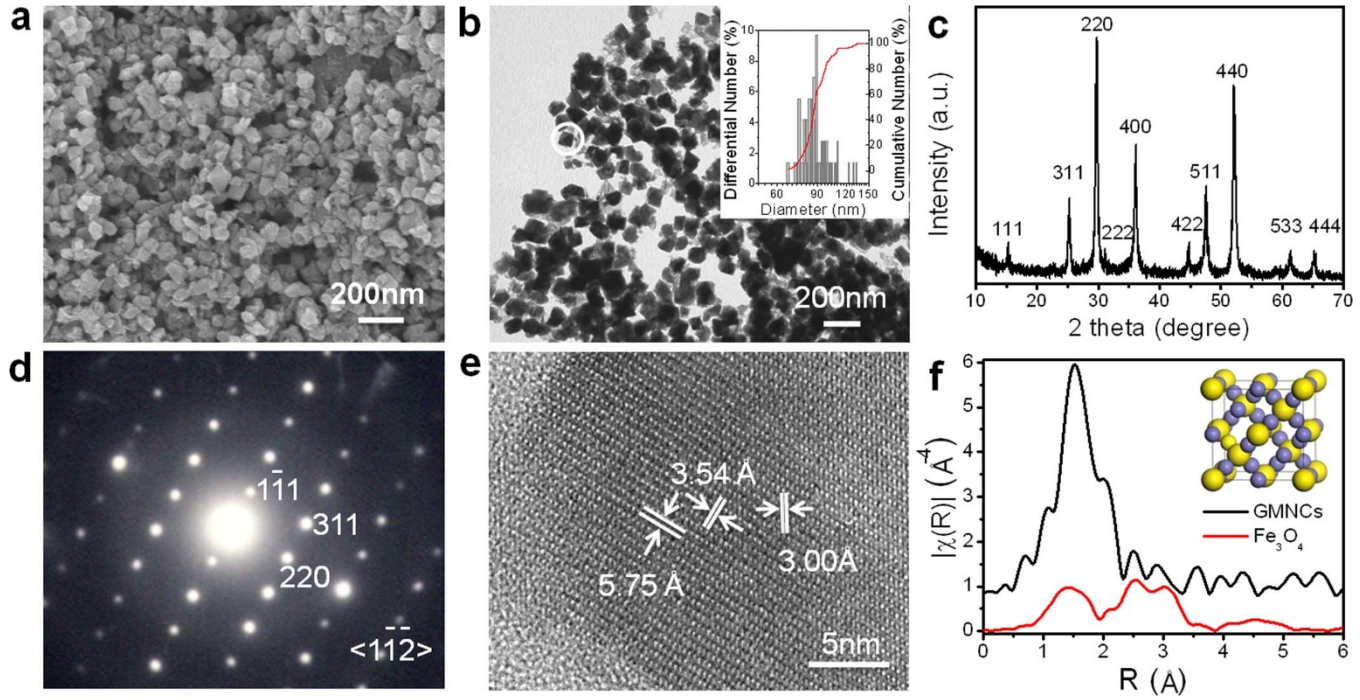

Figure 2 | Morphology and phase characterization of the magnetosome-like GMNCs. (a), FESEM and (b), TEM images show the morphologies and diameters of the as-prepared GMNCs synthesized in EG at 160°C for 2 h. Inset, the size histogram. (c), XRD pattern demonstrated the pure greigite phase. (d), SAED and (e), HRTEM are taken from the selected nanocrystal in (b), exhibiting high crystalline. (f), Fourier transformed XAFS functions in the R domain further illuminated the *fcc* Fe_3S_4 phase. Inset shows the cell structure of *fcc* Fe_3S_4.

(XRD) with 2θ range of 5°–65° (Fig. 2c). All the peaks have been indexed as a pure *fcc* phase of Fe_3S_4 structure with a lattice parameter of $a = 9.88$ nm (JCPDS No.16-0713), which was in good agreement with the literature value[5]. These GMNCs were well crystallized according to the selected-area electron diffraction (SAED) pattern in Fig. 2d and the corresponding high resolution transmission electron microscope (HRTEM) image in Fig. 2e, which were taken on the marked nanoparticle in Fig. 2b. The SAED pattern was taken along the $[1\ \bar{1}\ \bar{2}]$ direction. The lattice spacings of 5.8, 3.5, 3.0 Å in HRTEM are in good agreement with the value of the lattice spacings of the $(1\ \bar{1}\ 1)$, (220), (311) planes in SAED of the face-centered cubic (*fcc*) Fe_3S_4 phase. To further confirm the *fcc* structure, the synchrotron radiation technique[31] was utilized to obtain the iron *K*-edge XAFS spectra of the as-prepared GMNCs and the referenced Fe_3O_4 sample, as the detailed structural information of metal complexes can be derived from the XAFS spectra[32]. Fig. 2f showed the Fourier transformed XAFS functions of the GMNCs and Fe_3O_4 samples in the *R* domain, corresponding with the normalized iron *K*-edge XAFS spectrum (see Supplementary Information, Fig. S4). The results indicated the characteristic spectra of *fcc* crystallographic system[33], which confirmed the *fcc* phase of Fe_3S_4 structure (Inset in Fig. 2f). It can also be figured out that the shortest bond distance of Fe-S would be 1.5 Å.

The XRD pattern of our magnetosome-like GMNCs maintained in the air for more than six months has been identified (see Supplementary Information, Fig. S5), demonstrating their good stability in ambient environment. Detailed compositions of the products were exhibited through the XPS spectra (see Supplementary Information, Fig. S6), which also indicated the stoichiometry ratio of Fe and S atoms in these GMNCs. Fourier transform infrared (FTIR) spectra (Supplementary Information, Fig. S7a) showed the obvious difference of the as-prepared nanocrystals between with and without surface-coating, which nicely suggested the existence of β-CD and PEG molecules. Their corresponding XRD patterns (Supplementary Information, Fig. S7b) further illuminated the cooperation of these two organic molecules. UV-Vis spectrum (see Supplementary Information, Fig. S7c) clearly exhibited a strong absorption band centered at 280 nm and a very weak absorption at around 382 nm, which should also be attributed to the organic molecules. Thermogravimetric (TG) analysis (see Supplementary Information, Fig. S7d) indicated that there were about 17.3 wt% weight losses of the as-prepared GMNCs from room temperature to 1000°C. During the whole process, the mass losses should be owing to the adsorbent water and decomposition of the organic molecules in the GMNCs. In addition, due to the cooperation of these hydrophilic molecules, the as-synthesized GMNCs perform good hydrophilicity and water-solubility (Supplementary Information, Fig. S8).

Discussion

Recently, utilizing cyclodextrins to stablize nanoparticles have attracted great attention for drug delivery and diagnosis, which were generally recognized to be safe by the US Food and Drug Administration[34–36]. Additionally, PEGlyation has been defined as an effective way for the modification of nanomaterials. Based on this it was reasonable to assume that our artificially prepared GMNCs were biocompatible. Standard MTT analysis was carried out to evaluate the cellular biocompatibility of our GMNCs, and the results shown in Fig. S9 indicated that the good cytocompatibility even at a high concentration of 75.0 μg/mL. Interestingly, when HeLa cell (a common cancerous cell) was exposed to GMNCs, the cellular activity was a little bit lower than that of the mouse embryo fibroblast (MEF) cell. Moreover, hemolysis analysis was taken to demonstrate the blood compatibility, and the hemolysis of 2.1% after the incubation of GMNCs in blood at the concentration of 0.5 mg/mL was much lower than the limit of 5%. In addition, after 2 weeks i.v. injection of GMNCs into mice, blood counting (red blood cell, white bllod cell and platelets), enzyme activities measurement in serum (including alkaline phosphatase (ALP), alanine transaminase (ALT) and D-Lactate Dehydrogenase (D-LDH)), and histological analysis in

major organs (including liver, heart, lung, spleen and kidney) have been carried out. Noticeably, no evidence of adverse effect or injury can be induced by our GMNCs (see Supplementary Information, Fig. S10). Furthermore, the effective internalization of our GMNCs has also been confirmed by the observation of plentiful high contrast nanoparticles inside HeLa cell in comparision with the untreated control (see Supplementary Information, Fig. S11). All the biocompatibility results should be probably attributed to the coating of β-CD and PEG molecules, leading to the great potential in medical applications.

For further medical applications, we have firstly investigated the magnetic property of the GMNCs. It is reported that the iron sulfides exhibit interesting magnetic and electrical properties which are strongly related to the stoichiometric ratio between Fe and S as well as their crystalline structure[37], such as diamagnetic pyrite and marcasite (FeS_2), antiferromagnetic troilite (FeS) and ferromagnetic pyrrhotite ($Fe_{1-x}S$). Herein, magnetic investigation on all the magnetosome-like GMNCs was shown in Fig. 3a. Obviously, the magnetization of the GMNCs at room temperature was measured to be 49.3 emu per gram. Inset showed the magnified hysteresis loop, exhibiting about 139.9 Oe of coercive force, which was quite simiar to that of the previously reported iron oxides magnetosomes[38]. On the other hand, iron oxide nanomaterials as efficient MR contrast agents have been studied for a long time, and some of them, for example Feridex[39], have ever been permitted for commercial use. In addition, the iron oxide based bacterial magnetosome have been used to label macrophages[40]; meanwhile, single cells and transplanted pancreatic islets have also been imaged by magnetosome-like iron oxide nanocubes[41]. However, non-iron oxide based magnetic nanomaterials, including metal-alloy and oxide have served as novel magnetic resonance imaging agents in the past several years[42–44], and the iron sulfide should also be a reasonable candidate. Similarly, the great ability of our GMNCs for T_2-weighted MR imaging has also been demonstrated. In the T_2-weighted image of our GMNCs obtained from a clinic 3T MR scanner, the evident decrease of signal was observed with the double increase of iron concentration, indicating the shorten effect of T_2 value in the pseudo-color T_2 map as shown in Fig. 3b. The relaxivity of the GMNCs was calculated to be 94.8 $mM^{-1}s^{-1}$. After co-culture with our GMNCs overnight, obvious darkened effect of T_2-weighted signal was observed for HeLa cells in comparison with the control group (inset in Fig. 3c). These results indicated that the magnetosome-like GMNC would be the potential candidate as a novel MRI contrast agent.

In the past, biogenic magnetosomes have been successfully isolated and functionalized to load drugs for tumor therapy[45,46]. Due to the coating of oligosaccharide, our GMNCs can also absorb doxorubicin (Dox), which is a widely used anticancer drug. With the weight ratio of GMNCs to Dox varying from 1 : 1, 2 : 1, 5 : 1 to 20 : 1, the entrapment efficiency increased from 58.7, 62.7, 89.7 to 91.2%, whereas the loading efficiency of Dox decreased evidently from 58.7, 31.4, 17.9 to 4.6%. The results indicated that the optimal weight ratio for our GMNCs to load Dox should be 1 : 1 with an obviously high loading efficiency of Dox for further in vivo antitumor research. In vivo evaluations of our GMNCs mediated inhibition of tumor growth were performed in S180 sarcoma bearing mice (Fig. 3d). In comparison with control group, the groups which were injected with 2.5 mg/kg of greigite MNCs and 2.5 mg/kg of Dox i.v. showed the reduced tumor weight of about 91.2 and 69.0%, respectively. When the NCs loading with Dox was injected in vivo i.v. at the concentration of

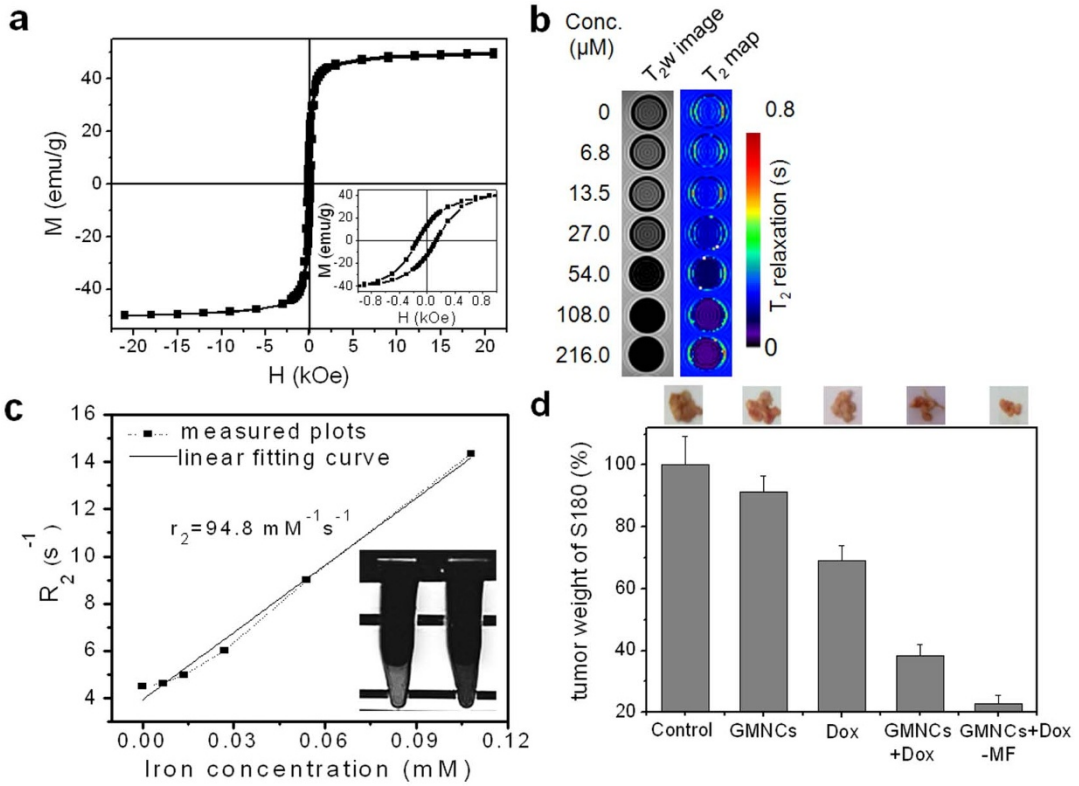

Figure 3 | Magnetic property, magnetic resonance imaging (MRI) and cancer inhibition of the magnetosome-like GMNCs. (a), Magnetization hysteresis loop of the as-prepared GMNCs at room temperature. Inset showed the magnified hysteresis loop in the coercive field from −1000 Oe to 1000 Oe. (b), T_2w image and pseudocolour T_2 map of our GMNCs. (c), plot of R_2 ($1/T_2$) over iron concentration (mM) of GMNCs, and the slope via linear fitting indicate the relaxivity (r_2). Inset is HeLa cellular T_2w image exposed to our GMNCs (left: MNCs group; right: control group). (d), Growth inhibition effect in murine S180 sarcoma model of the sample. The photos and weight ratios of tumor tissue from mice treated with normal saline (control group), GMNCs, Dox at low concentration, and GMNCs loading with Dox (without and with the guidance of external magnetic field), respectively.

2.5 mg Dox per kilogram of body weight, the growth of S-180 sarcoma was obviously inhibited. Moreover, enhanced inhibition effect of the sarcoma growth was observed under the guidance of external magnetic field, and particularly the weight of remaining tumor was only 22.8% of control group due to the magnetic field mediated release of Dox in targeted tumor areas from the GMNCs.

In summary, a facile solvothermal procedure for large scale synthesis of hydrophilic magnetosome-like GMNCs has been successfully reported here for the first time. Due to the presence of β-CD and PEG molecules, the obtained GMNCs with pure greigite phase possessed uniform size, good crystallization and stabilization, which were similar to the natural bacterial magnetosomes. Their perfect biocompatibility, MRI ability, and drug delivery for inhibiting the growth of cancer *in vivo* have been exhibited as well. As an important progress in magnetic nanomaterials, it is reasonable that the obtained magnetosome-like GMNCs should have promising potentials in magnetic separation, detection, catalysis in the future. In addition, combining these GMNCs with many other functional nanocomponents to fabricate multiple-functional nanocomposites[47,48] should be feasile and would be highly valuable. Furthermore, learning and mimicing the energy-saving bio-synthesis process have attracted our great attention[22,49,50], and we will focus on the design of bioreactor to produce nanomaterials, especially the magnetosome-like greigite.

Methods

Materials. All chemicals are analytical grade. Iron(III) acetylacetonate ($Fe(acac)_3$) was purchased from Alfa-Aesar (U.S.A.); thioacetamide (TAA), ethylene glycol (EG), α, β, γ-cyclodextrin (α, β, γ-CD), polyethylene glycol (PEG), sodium dodecyl sulfate (SDS), polyvinylpyrrolidone (PVP), oleic acid (OA), hexadecyl trimethyl ammonium bromide (CTAB), trioctylphosphine oxide (TOPO), polyacrylamide (PAM), L-Cystine, and dimethylsulfoxide (DMSO) were purchased from Shanghai Chemical Reagent Co. Ltd (China). Doxorubicin, MTT and agarose were purchased from Sangon Biotech (Shanghai) Co., Ltd (China). All reagents were used as received without further purification.

Synthesis of the magnetosome-like GMNCs. The massive water soluble GMNCs were synthesized from a polar solvent and the synthesis was based on a solvothermal method. In a typical procedure, 0.25 mmol of iron(III) acetylacetonate, 0.25 mmol of β-cyclodextrin and 0.5 mmol polyethylene glycol were dissolved in ethylene glycol (20 ml) until the temperature was up to 160°C and the mixture was kept for 30 min at this temperature. At this stage, turbid yellow suspension came into being. Then 0.0260 g thioacetamide dissolved in 5 ml of ethylene glycol were injected slowly into the above mixture and black sediment immediately formed. The mixed solution was kept stirring for 2 h at the temperature. Noticeably, the whole procedure was carried out in the atmosphere of flowing nitrogen.

Biocompatibility test. For MTT analysis, HeLa and the MEF (mouse embryo fibroblast) cells were chosen to expose to greigite MNC solution with a series of concentrations (0–75 μg/mL) for 24 h. Then the medium was replaced, and 20 μL of MTT solution (4 mg/mL) was added for a further co-incubation of 4 h. After remove of MTT solution, 100 μL of DMSO was added to dissolve the formed purple formazan for determination on a spectrophotometric microplate reader (Bio-tek ELX800, USA). For hemolysis evaluation, human blood was incubated with 0.5 mg GMNCs/mL normal saline solution with DI water and normal saline served as positive and negative control. After 1 h incubation at 37°C, the samples were centrifuged to remove blood cells, and the optical density (OD) of the supernatant solution was then measured at 545 nm to calculate the percentage hemolysis. For blood and histological analysis, after 2weeks of the i.v. injection with GMNCs at the concentration of 2.5 mg/kg, blood cells of mice were counted, and enzyme activities in serum including ALT, ALP and D-LDH were measured, while the histological sections of major organs including liver, heart, spleen, lung and kidney were obtained and stained by Hematoxylin and eosin (H&E) staining.

MR imaging. Magnetic resonance imaging (MRI) of GMNCs with the concentration increasing from 0 to 128.0 μg/ml in 0.5% agarose gel, was performed on a Siemens 3T Trio Tim clinical MR scanner containing a knee coil. TSE (Turbo spin echo) sequence was utilized to obtain the T_2-weighted images (TR: 5000 ms, TE: 89 ms, slice thickness: 5 mm), and T_2 map was obtained on the Siemens workstation. Through linear fitting of R_2 ($1/T_2$) to molar concentration of iron, the relaxation ratio (r2) of the greigite MNCs was calculated as the slope.

In vivo tumor inhibition Animals and tumor model. Healthy Kunming male mice (aged 6–8 weeks) purchased from Experimental Animal Center of Anhui Medical University were used to establish tumor model in the right forelimb. After the S180 ascites injection subcutaneously, all the 50 S180 tumor-bearing mice were randomly divided into five groups, including control group, GMNCs group, Dox group and GMNCs + Dox group with/without external magnetic field to investigate the in vivo tumor inhibiting effect, and the materials for chemotherapy were injected intravenously (i.v.) at the second, fourth and sixth day, respectively. One week later, the subcutaneous sarcoma tumors were taken out and weighted to evaluate the anti-tumor effect.

Instruments. X-ray diffraction (XRD) was examined on a Philips X'Pert PRO SUPER X-ray diffractometer. X-ray photoelectron spectra (XPS) were recorded on ESCALAB MK II. Scanning electron microscopy (SEM) was carried out on JEOL-6700F. Transmission electron microscope (TEM), high-resolution transmission electron microscope (HRTEM) and selected area electron diffraction (SAED) patterns were performed on JEOL-2010 transmission electron microscope with an acceleration voltage of 200 kV. FT-IR spectra were measured on a Bruker Vector-22 FT-IR spectrometer. Thermogravimetric analysis (TGA) and differential thermal analysis (DTA) were carried out on a TGA-60H thermal analyzer. UV-Vis absorption spectrum was recorded by a Shimadzu UV-2250 instrument. The magnetic measurements were carried out with a superconducting quantum interference device (SQUID) magnetometer. The *in situ* XAFS measurements at Fe K-edge was performed in transmission mode at NW10A station in PF-AR (Photon Factory Advanced Ring for Pulse X-ray, Japan) and U7C XAFS station in NSRL (National Synchrotron Radiation Laboratory, P. R. China).

1. El-Jaick, L. J., Acosta-Avalos, D., De Souza, D. M., Wajnberg, E. & Linhares, M. P. Electron paramagnetic resonance study of honeybee Apis mellifera abdomens. *Eur. Biophys. J.* **29**, 579–586 (2001).
2. Zoeger, J., Dunn, J. R. & Fuller, M. Magnetic material in the head of the common pacific dolphin. *Science* **213**, 892–894 (1981).
3. Blakemore, R. P. Magnetotactic bacteria. *Science* **190**, 337–379 (1975).
4. Lu, Y., Dong, L., Zhang, L. C., Su, Y. D. & Yu, S. H. Biogenic and biomimetic magnetic nanosized assemblies. *Nano Today* **7**, 297–315 (2012).
5. Mann, S., Sparks, N. H. C., Frankel, R. B., Bazylinski, D. A. & Jannasch, H. W. Biomineralization of ferrimagnetic greigite (Fe_3S_4) and iron pyrite (FeS_2) in a magnetotactic bacterium. *Nature* **343**, 258–261 (1990).
6. Farina, M., Esquivel, D. M. S. & Debarros, H. Magnetic iron-sulfur crystals from a magnetotactic microorganism. *Nature* **343**, 256–258 (1990).
7. Faivre, D. & Schueler, D. Magnetotactic bacteria and magnetosomes. *Chem. Rev.* **108**, 4875–4898 (2008).
8. Posfai, M. & Dunin-Borkowski, R. E. Sulfides in biosystems *Rev. Mineral. Geochem.* **61**, 679–714 (2006).
9. Hu, J. M., Li, Z., Chen, L. Q. & Nan, C. W. High-density magnetoresistive random access memory operating at ultralow voltage at room temperature. *Nat. Commun.* **2**, 553 (2011).
10. Polshettiwar, V. *et al.* Magnetically Recoverable Nanocatalysts. *Chem. Rev.* **111**, 3036–3075 (2011).
11. Lee, J. H. *et al.* Exchange-coupled magnetic nanoparticles for efficient heat induction. *Nat. Nanotechnol.* **6**, 418–422 (2011).
12. Kim, B. H. *et al.* Large-Scale Synthesis of Uniform and Extremely Small-Sized Iron Oxide Nanoparticles for High-Resolution T-1 Magnetic Resonance Imaging Contrast Agents. *J. Am. Chem. Soc.* **133**, 12624–12631 (2011).
13. Kievit, F. M. & Zhang, M. Q. Surface Engineering of Iron Oxide Nanoparticles for Targeted Cancer Therapy. *Acc. Chem. Res.* **44**, 853–862 (2011).
14. Ho, D., Sun, X. L. & Sun, S. H. Monodisperse Magnetic Nanoparticles for Theranostic Applications. *Acc. Chem. Res.* **44**, 875–882 (2011).
15. Ge, J. P. & Yin, Y. D. Responsive Photonic Crystals. *Angew. Chem. Int. Ed.* **50**, 1492–1522 (2011).
16. Skinner, B. J., Erd, R. C. & Grimaldi, F. S. Greigite, the thio-spinel of iron; a new mineral. *Am. Miner.* **49**, 543–555 (1964).
17. Paolella, A. *et al.* Charge Transport and Electrochemical Properties of Colloidal Greigite (Fe_3S_4) Nanoplatelets. *Chem. Mater.* **23**, 3762–3768 (2011).
18. Chang, Y. S., Savitha, S., Sadhasivam, S., Hsu, C. K. & Lin, F. H. Fabrication, characterization, and application of greigite nanoparticles for cancer hyperthermia. *J. Colloid Interface Sci.* **363**, 314–319 (2011).
19. Apostolova, R. D., Kolomoets, O. V. & Shembel, E. M. Electrolytic Iron Sulfi des for Thin-Layer Lithium-Ion Batteries. *Russ. J. Appl. Chem.* **82**, 1939–1943 (2009).
20. Hunger, S. & Benning, L. G. Greigite: a true intermediate on the polysulfide pathway to pyrite. *Geochem. Trans.* **8**, 1 (2007).
21. Vanitha, P. V. & O'Brien, P. Phase control in the synthesis of magnetic iron sulfide nanocrystals from a cubane-type Fe-S cluster. *J. Am. Chem. Soc.* **130**, 17256–17257 (2008).
22. Lefevre, C. T. *et al.* A cultured greigite-producing magnetotactic bacterium in a novel group of sulfate-reducing bacteria. *Science* **334**, 1720–1723 (2011).
23. He, Z. B., Yu, S. H., Zhou, X. Y., Li, X. G. & Qu, J. F. Magnetic-field-induced phase-selective synthesis of ferrosulfide microrods by a hydrothermal process: microstructure control and magnetic properties. *Adv. Funct. Mater.* **16**, 1105–1111 (2006).
24. Chen, X. Y., Zhang, X. F., Wan, J. X., Wang, Z. H. & Qian, Y. T. Selective fabrication of metastable greigite (Fe_3S_4) nanocrystallites and its magnetic properties through a simple solution-based route. *Chem. Phys. Lett.* **403**, 396–399 (2005).

25. Zhou, J., Hu, Z. G., Munck, E. & Holm, R. H. The cuboidal Fe_3S_4 cluster: Synthesis, stability, and geometric and electronic structures in a non-protein environment. *J. Am. Chem. Soc.* **118**, 1966–1980 (1996).
26. Ma, J. M. *et al*. Ionic liquid-modulated synthesis of ferrimagnetic Fe_3S_4 hierarchical superstructures. *Chem. Commun.* **46**, 5006–5008 (2010).
27. Beal, J. H. L. *et al*. Synthesis and Comparison of the Magnetic Properties of Iron Sulfide Spinel and Iron Oxide Spinel Nanocrystals. *Chem. Mater.* **23**, 2514–2517 (2011).
28. Khan, A. R., Forgo, P., Stine, K. J. & D'Souza, V. T. Methods for selective modifications of cyclodextrins. *Chem. Rev.* **98**, 1977–1996 (1998).
29. Naresh, M., Das, S., Mishra, P. & Mittal, A. The chemical formula of a magnetotactic bacterium. *Biotechnol. Bioeng.* **109**, 1205–1216 (2012).
30. Naresh, M. *et al*. NSOM/HRTEM Characterization of Biologically Derived Cubo-Octahedral Nanomagnets. *IEEE Trans. Magn.* **45**, 4861–4864 (2009).
31. Hendrickson, W. A. Determination of macromolecular structures from anomalous diffraction of synchrotron. *Science* **254**, 51–58 (1991).
32. Neidig, M. L. *et al*. Ag K-edge EXAFS analysis of DNA-templated fluorescent silver nanoclusters: insight into the structural origins of emission tuning by DNA sequence variations. *J. Am. Chem. Soc.* **133**, 11837–11839 (2011).
33. Krylov, A. S., Poliakoff, J. F. & Stockenhuber, M. An hermite expansion method for EXAFS data treatment and its application to Fe K-edge spectra. *Phys. Chem. Chem. Phys.* **2**, 5743–5749 (2000).
34. Zhao, J. *et al*. Highly sensitive identification of cancer cells by combining the new tetrathiafulvalene derivative with a beta-cyclodextrin/multi-walled carbon nanotubes modified GCE. *Analyst* **135**, 2965–2969 (2010).
35. Park, C. *et al*. Cyclodextrin-covered gold nanoparticles for targeted delivery of an anti-cancer drug. *J. Mater. Chem.* **19**, 2310–2315 (2009).
36. Li, J. & Loh, X. J. Cyclodextrin-based supramolecular architectures: Syntheses, structures, and applications for drug and gene delivery. *Adv. Drug Delivery Rev.* **60**, 1000–1017 (2008).
37. Rickard, D. & Luther, G. W. I. Chemistry of iron sulfides. *Chem. Rev.* **107**, 514–562 (2007).
38. Staniland, S. *et al*. Controlled cobalt doping of magnetosomes in vivo. *Nat. Nanotechnol.* **3**, 158–162 (2008).
39. Barnett, B. P. *et al*. Magnetic resonance-guided, real-time targeted delivery and imaging of magnetocapsules immunoprotecting pancreatic islet cells. *Nat. Med.* **13**, 986–991 (2007).
40. Hartung, A. *et al*. Labeling of macrophages using bacterial magnetosomes and their characterization by magnetic resonance imaging. *J. Magn. Magn. Mater.* **311**, 454–459 (2007).
41. Lee, N. *et al*. Magnetosome-like ferrimagnetic iron oxide nanocubes for highly sensitive MRI of single cells and transplanted pancreatic islets. *Proc. Natl. Acad. Sci. U. S. A.* **108**, 2662–2667 (2011).
42. Lu, Y. *et al*. MnO Nanocrystals: A Platform for Integration of MRI and Genuine Autophagy Induction for Chemotherapy. *Adv. Funct. Mater.* **23**, 1534–1546 (2013).
43. Lu, Y. *et al*. Magnetic Alloy Nanorings Loaded with Gold Nanoparticles: Synthesis and Applications as Multimodal Imaging Contrast Agents. *Adv. Funct. Mater.* **20**, 3701–3706 (2010).
44. Jun, Y. W., Lee, J. H. & Cheon, J. Chemical design of nanoparticle probes for high-performance magnetic resonance imaging. *Angew. Chem. Int. Ed.* **47**, 5122–5135 (2008).
45. Sun, J. B. *et al*. Preparation and anti-tumor efficiency evaluation of doxorubicin-loaded bacterial magnetosomes: magnetic nanoparticles as drug carriers isolated from magnetospirillum gryphiswaldense. *Biotechnol. Bioeng.* **101**, 1313–1320 (2008).
46. Li, X. *et al*. Bacterial magnetic particles (BMPs)-PEI as a novel and efficient non-viral gene delivery system. *J. Gene. Med.* **9**, 679–690 (2007).
47. Jin, Y., Jia, C., Huang, S. W., O'Donnell, M. & Gao, X. Multifunctional nanoparticles as coupled contrast agents. *Nat. Commun.* **1**, 41 (2010).
48. Gao, J., Gu, H. & Xu, B. Multifunctional Magnetic Nanoparticles: Design, Synthesis, and Biomedical Applications. *Acc. Chem. Res.* **42**, 1097–1107 (2009).
49. Stuerzenbaum, S. R. *et al*. Biosynthesis of luminescent quantum dots in an earthworm. *Nat. Nanotechnol.* **8**, 57–60 (2013).
50. Naresh, M., Hasija, V., Sharma, M. & Mittal, A. Synthesis of Cellular Organelles Containing Nano-Magnets Stunts Growth of Magnetotactic Bacteria. *J. Nanosci. Nanotechnol.* **10**, 4135–4144 (2010).

Acknowledgments

S.H.Y. acknowledges acknowledge the funding support from the National Basic Research Program of China (Grants 2010CB934700, 2013CB931800), the National Natural Science Foundation of China (Grants 91022032, 91227103, 21061160492, J1030412), Chinese Academy of Sciences (Grant KJZD-EW-M01-1), International Science & Technology Cooperation Program of China (Grant 2010DFA41170), the Fundamental Research Funds for the Central Universities (WK2060190016, WK2060190021), the China Postdoctoral Science Foundation funded project (BH2060190035, 2060190040) and Anhui Provincial Natural Science Foundation of China (No. 11040606M193). Heartfelt thanks to Dr. Ce Shi at the University of Southern California (USA), and Xiang-Hua Huang, and Jun-Tong Gu at Anhui Univerisity of Traditional Chinese Medicine for their support in this work.

Author contributions

M.F. and Y.L. performed the whole work of design, synthesis, characterization of the GMNCs and research of biomedical applications. S.H.Y. supervised the project, and conceived the experiments, analyzed the results and wrote the paper. M.F. and Y.L. contributed to the data analyses, and preparation of the manuscript. Y.Y. and M.Z. performed the synthesis. Y.J.X. performed the MR measurement. H.L.G., L.D. and W.P.X. performed the antitumor investigation in vivo.

Additional information

Supplementary information accompanies this paper at http://www.nature.com/scientificreports

Competing financial interests: The authors declare no competing financial interests.

How to cite this article: Feng, M. *et al*. Bioinspired greigite magnetic nanocrystals: chemical synthesis and biomedicine applications. *Sci. Rep.* **3**, 2994; DOI:10.1038/srep02994 (2013).